TECHNICAL REPORT ARLCD-TR-81044

CARS SPECTROSCOPY OF GUN PROPELLANT FLAMES— HIGHER HOT BAND AND CONCENTRATION EFFECTS

L. E. HARRIS

FEBRUARY 1982

US ARMY ARMAMENT RESEARCH AND DEVELOPMENT COMMAND
LARGE CALIBER
WEAPON SYSTEMS LABORATORY
DOVER, NEW JERSEY

The views, opinions, and/or findings contained in this report are those of the author and should not be construed as an official Department of the Army position, policy or decision, unless so designated by other documentation.

Destroy this report when no longer needed. Do not return to the originator.

The citation in this report of the names of commercial firms or commercially available products or services does not constitute official endorsement or approval of such commercial firms, products, or services by the US Government.

UNCLASSIFIED

SECURITY CLASSIFICATION OF THIS PAGE *(When Date Entered)*

REPORT DOCUMENTATION PAGE		READ INSTRUCTIONS BEFORE COMPLETING FORM
1. REPORT NUMBER Technical Report ARLCD-TR-81044	2. GOVT ACCESSION NO.	3. RECIPIENT'S CATALOG NUMBER
4. TITLE *(and Subtitle)* CARS SPECTROSCOPY OF GUN PROPELLANT FLAMES-- HIGHER HOT BAND AND CONCENTRATION EFFECTS		5. TYPE OF REPORT & PERIOD COVERED 6. PERFORMING ORG. REPORT NUMBER
7. AUTHOR(s) L. E. Harris		8. CONTRACT OR GRANT NUMBER(s)
9. PERFORMING ORGANIZATION NAME AND ADDRESS ARRADCOM, LCESL Applied Sciences Div (DRDAR-LCA-G) Dover, NJ 07801		10. PROGRAM ELEMENT, PROJECT, TASK AREA & WORK UNIT NUMBERS
11. CONTROLLING OFFICE NAME AND ADDRESS ARRADCOM, TSD STINFO Div, (DRDAR-TSS) Dover, NJ 07801		12. REPORT DATE February 1982 13. NUMBER OF PAGES 38
14. MONITORING AGENCY NAME & ADDRESS*(if different from Controlling Office)*		15. SECURITY CLASS. *(of this report)* Unclassified 15a. DECLASSIFICATION/DOWNGRADING SCHEDULE

16. DISTRIBUTION STATEMENT *(of this Report)*

Approved for public release; distribution unlimited.

17. DISTRIBUTION STATEMENT *(of the abstract entered in Block 20, if different from Report)*

18. SUPPLEMENTARY NOTES

19. KEY WORDS *(Continue on reverse side if necessary and identify by block number)*

Propellant
Combustion
Flame
CARS
Spectroscopy

20. ABSTRACT *(Continue on reverse side if necessary and identify by block number)*

Nitrogen Coherent Anti-Stokes Raman Scattering (CARS) spectra from nitrate-ester propellant flames contain several features not reported in nitrogen CARS spectra from other flames. Prominent among these features is a high intensity peak (30% maximum) 30 cm(-1)to the low energy side of the first hot band. Nitrogen CARS spectra from air/argon mixture containing from 1% to 30% air changed substantially with concentration but agreed with calculated spectra to better than 6%. Nitrogen CARS spectra from propane/air flames of

(cont)

DD FORM 1 JAN 73 1473 EDITION OF 1 NOV 65 IS OBSOLETE

UNCLASSIFIED

SECURITY CLASSIFICATION OF THIS PAGE *(When Data Entered)*

20. Abstract (cont)

various equivalence ratios showed a resolved second hot band, Q(32) at 2,269 cm(-1) and the presence of the third hot band, Q(43), near 2,241 cm(-1). Temperatures determined from Q(32) agreed, within experimental error, with those determined with Q(10) at 2,296 cm(-1). Temperature trends for the various equivalence ratios agreed with thermochemical predictions, allowing the accuracy to be assessed at better than 5%. The good agreement of nonplanar and planar BOXCARS validated the earlier planar BOXCARS measurements. Nitrogen CARS calculations agreed well with experimental propellant spectra at the 10% nitrogen concentration expected from thermochemical calculations. The calculated spectra show the presence of Q(32) near 30% maximum intensity as seen in the propellant spectra.

CONTENTS

TABLES

FIGURES

INTRODUCTION

Measurements of temperature and concentration spatial profiles in propellant and related laboratory flames should provide experimental results needed to identify the controlling mechanisms of propellant combustion. These measurements are difficult to make with conventional methods since propellant flames are often transient, incandescent, and particle-laden. Coherent Anti-Stokes Raman Scattering (CARS), due to its high intensity and coherent nature, provides a means of probing propellant flames. The CARS signal can be generated from a spatially, well defined region in the flame on the order of 1 mm^3 within the time duration of the laser pulse. CARS involves the interaction of two high intensity laser beams, the pump and Stokes beams, at angular frequencies ω_ℓ and ω_s, respectively. When ω_ℓ and ω_s are separated by a Raman resonance frequency, CARS, ω_{as} is generated at the anti-Stokes frequency. CARS signal strength is proportional to the square of the modulus of the third-order electric susceptibility, $/\chi^{(3)}/$. The susceptibility is the sum of a resonant, χ_r, and nonresonant term, χ_{nr}. χ_r can be expanded into a real and imaginary term.

$$/\chi^{(3)}/^2 = /\chi_r' + i\chi_r'' + \chi_{nr}/^2 \tag{1}$$

χ_r' and χ_r'' have dispersive and resonant line shapes, respectively; therefore, at low concentration the CARS lineshape becomes dispersive.

$$/\chi^{(3)}/^2 = /\chi_r' \chi_{nr} + \chi_{nr}^2/ \tag{2}$$

Nitrogen CARS spectra have been reported for nitrate-ester propellant flames (ref 1 through 3). The propellant spectra contained several features that had not been reported in nitrogen CARS spectra from other flames. The novel features in the propellant nitrogen CARS spectra can be attributed to the lower concentration of nitrogen, the high temperature of the flame, and the lower resolution necessitated by the low intensity of the spectra. Prominent among the novel features was a high intensity (30% maximum) peak 30 cm^{-1} to the low energy side of the first hot band. This peak had not been reported in previous investigations on flames. To determine the nature of the novel spectral features, the following investigations were undertaken:

1. Nitrogen CARS spectra from air/argon mixtures with nitrogen at concentrations near that in the propellant flame (10%).

2. Nitrogen CARS spectra from propane/air flames of various equivalence ratios with emphasis on the behavior of the second hot band. Thermochemical calculations were performed to assess the accuracy of the experimentally determined temperatures.

EXPERIMENTAL

CARS spectra were generated using apparatus with both planar and nonplanar BOXCARS (ref 4) phasematching (fig. 1), using the apparatus shown in figure 2. The pump laser beam, ω_ℓ is produced by a Quanta-Ray DCR-1A Nd/YAG laser. The output of the Nd/YAG laser at 1.06 microns (700 mj) is doubled to generate the pump beam, ω_ℓ, at 5,320 Å (250 mj) with a bandwidth of about 1 cm^{-1}. The pump beam is separated from the primary beam using prisms. Forty percent of the pump beam is split off (BS_1) to pump a dye laser to generate the Stokes beam, ω_s. The dye laser is operated broadband to produce 30 mj centered at 6,070 Å with a bandwidth of about 150 cm^{-1}. To achieve BOXCARS geometry, the pump is split using a 50% beamsplitter, BS_2. In planar BOXCARS, the ω_ℓ beam is reflected from a dichroic (DC) which transmits the stokes beam, and ω_ℓ' is separately reflected along another path so that the pump beams are separated at the focusing lens. The planar BOXCARS signal, ω_{as}, which is generated along ω_ℓ, is isolated by prism and spatial filtering. In nonplanar BOXCARS, ω_s is introduced below the plane of ω_ℓ at the focusing lens to produce a spatially isolated ω_{as} which is focused onto the slits of a monochromator fitted with a PAR SIT detector. The signal from the detector is sent to an OMA2 for processing.

In these experiments a 200-mm focusing lens was used with a pump beam crossing angle of 5° in planar BOXCARS. In nonplanar BOXCARS, the ω_ℓ, ω_ℓ', and ω_s beams are situated on a circle of 1-inch radius at the focusing lens with ω_ℓ and ω_ℓ' in the horizontal plane and ω_s in the vertical plane. A 1/4-meter monochromator equipped with a 1,800 line/mm grating and 100-micron slits was used for dispersal of ω_{as}. Neon spectral lines were used to determine the resolution and wavelength calibration of the monochrometer.

RESULTS

Temperature is determined by comparison of the experimental N_2 spectra with spectra calculated according to the procedure given by Hall (ref 5) using parameters given in references 5 through 7. The spectral parameters of ω_s were determined by flowing argon with some admixture of air through the burner to generate nonresonant CARS spectra which mirrors the spectral shape of ω_s. This spectra, in addition to providing the spectral parameters of ω_s illustrates the dependence of CARS spectra on concentration. CARS spectra from room temperature air/argon mixtures containing from 1% to 100% air are shown in figures 3 and 4. A comparison of calculated and experimental spectra in a 9% and 20% air/argon mixture is shown in figures 5 and 6, respectively. The ratio of the maximum intensities at Q_{10} and the nonresonant susceptibility is a direct measure of the concentration. Experimental and calculated maximum Q_{10} to nonresonant susceptibility ratio are given in table 1 and shown in figure 7. The agreement between theory and experimental is given in table 1 as 6.1%. The depth of the dip goes to increasingly larger intensity as the concentration decreases. A similar effect of concentration on CARS CO spectra was observed by Eckbreth (ref 4). The spectrum shown in figure 8 was determined using nonplanar BOXCARS with a slit width of 6.4 cm^{-1} and 2.38 cm^{-1} per channel as determined from the room temperature N_2 CARS spectrum shown in figures 5, 6, and 7. The spectral parameters determined for ω_s from

spectra similar to that in figure 5 were ω_s^{max} at 16,500 cm^{-1} with full width at half height (FWHH) of 130 cm^{-1}. These experimental parameters pertain to all the other reported nonplanar BOXCARS spectra. The experimentally determined parameters were used to generate CARS spectra with temperatures varying from 1,500 to 3,000 K (at 250-K intervals) which are shown in figure 9. The Q_{10}, Q_{21}, and Q_{32} peaks are seen to be clearly resolved at near to 2,325, 2,296, and 2,269 cm^{-1}, respectively. The bands shift slightly to the red as the temperature is raised. A shoulder near 2,241 cm^{-1}, attributable to Q_{43}, is seen to be almost resolved at 3,000 K. The average calculated separation between peaks is 28 cm^{-1}. The relative height of the Q_{10} peak determined experimentally was previously used to determine temperature from the calculated spectra (ref 4). Calculations made at small intervals (20 K) such as shown in figure 10 are, in practice, used to determine temperature.

Measurements of N_2 CARS spectra were made immediately above the reaction zone on the centerline of the burner with both nonplanar and planar BOXCARS. The nonplanar results were obtained at fuel/air equivalence ratios of 1.02, 0.81, and 1.27. The 1.02 and 0.81 equivalence ratio results are shown in figures 11 and 12, respectively, along with the calculated spectra. (The 1.27 equivalence ratio results look very similar to the 0.81 results.) The planar results are given in figure 13.

The Q_{32} peak is resolved and occurs at the calculated frequency. The Q_{43} is not clearly resolved but can be identified as occurring at the calculated position.

The results of the thermochemical calculations performed with the NASA-LEWIS computer code at the experimental equivalence ratios are given in table 2. The temperatures determined from the Q_{21} and Q_{32} peaks, T_{21} and T_{32}, respectively, are given in table 3. The temperatures determined from two different spectra for the equivalence ratio 1.02 showed that the precision of the method was quite good. The agreement between T_{21} and T_{32} was within the accuracy of the experimental data; however, T_{32} was systematically lower than T_{21}. This may result from slight inaccuracies in the ω_s parameters. Since T_{21} and T_{32} agreed within the accuracy of the data, no attempt was made to vary the ω_s parameters. A comparison of the experimental and thermochemically calculated temperatures is given in table 4. The experimentally determined temperatures are lower than the calculated adiabatic flame temperatures by about 10% on average. This is attributable to heat loss by radiation, thermal conduction, or diffusion which vary with burner design. The magnitude of the error is consistent with previous studies (ref 8). The error determined from the normalized temperatures (assuming constant percentage heat loss) is consistent with the known errors in CARS temperature determination and the flowmeters. The error is predominately in the flowmeters since the precision of CARS was shown above to be better.

Temperatures were also determined at the equivalence ratio of 1.02 with the planar BOXCARS configuration. The ω_s parameters were ω_s^{max} at 16,497 cm^{-1} with a width of 153 cm^{-1}. The slit width determined from the room temperature spectra was 9.6 cm^{-1} with 2.336 cm^{-1} per channel. A comparison of the planar and nonplanar T_{21} and T_{32} temperatures is shown in table 5. The agreement is very good considering the substantial changes made in the apparatus.

DISCUSSION

The high temperature and low concentration (less than 30%) of each product in propellant flames introduce features of N_2 CARS not previously reported. In addition, to attain the required intensity, lower resolution than that used in other studies was used.

Concentration as shown in figures 3, 4, 5, and 6 alters the appearance of N_2 CARS spectra at room temperature. The effect of concentration at 2,500 K is shown in figure 14. At higher concentration of room temperature spectra, the calculated maximum intensity falls as the square of the concentration. However, at high temperatures the steepness of the decline of the signal with concentration begins to moderate at 50% air as opposed to room temperature where moderation does not begin to occur until 5% air is reached. This difference occurs because the high temperature spectra is spectrally wider than the room temperature spectra. As a consequence, the maximum intensity at high temperature is less relative to the nonresonant susceptibility than at low temperatures. At the 10% level, the signal is decreased from the 100% level by factors of 85 and 25 at 298 and 2,500 K, respectively. This lessening of the square root dependence of intensity on concentration makes possible CARS measurements in flames at lower levels of the concentration of products.

The Q_{32} hot band is much more sensitive to concentration than Q_{21}. At the 50% level, Q_{32} has more than doubled in intensity while Q_{21} has only increased by a few percent. Thus, high temperature and low concentration result in high intensity of Q_{32} in the previously reported propellant spectra. The results given in tables 3 through 5 establish the utility of Q_{32} for measurement of temperature. The results in figure 14 indicate that Q_{32} is useful for estimation of the concentration in the range 10% to 100%, given an approximate temperature from Q_{10}. Below 10%, if a spectrum can be obtained, the depth of the dip on the high energy side of Q_{10} is useful for estimation of the concentration. These initial estimates of temperature and concentration should be used as input to a least-squares routine to accurately determine temperature and concentration from the spectrum. In the situation where all species are present below the 30% level, it becomes necessary to determine temperature and concentration simultaneously.

The results obtained in comparison of planar and nonplanar BOXCARS indicate that configuration can have an effect on the resolution of the observed spectra. Nonplanar and planar BOXCARS were observed to give spectral resolutions of 6.4 and 9.6 cm^{-1}, respectively. This may be due to some distortion of the spectrum resulting from the additional optical elements in planar BOXCARS. It is also possible that the positioning of the CARS signal was not optimized in the planar BOXCARS configuration. The intensity of the CARS signal was higher in the planar configuration which may have some effect on the resolution. Since the spectra and temperatures were the same for planar and nonplanar BOXCARS, no clipping by the slit of the prism-dispersed planar BOXCARS signal is evident. However, the cm^{-1}/channel of the planar BOXCARS signal was reduced from the 2.34 to 2.20 to adequately match the spectrum. This was not necessary in nonplanar BOXCARS and may reflect the additional dispersion due to the prism used in planar BOXCARS.

The spectral features observed in propane/air flames and air/ar mixtures can be used to interpret the previously reported propellant spectra which are intermediate between the 25% air (18% N_2) and 50% air (35% N_2) spectra shown in figure 14. The calculated concentration of N_2 in the propellant was 10%. However, the nonresonant susceptibility in the propellant flame is higher than the value used for the propane/air flame; this would reduce the computed concentration. Differences in spectral properties of ω_s may account for the remaining difference. Alternately there could be some initial mixing in of air. Further work will be needed to resolve this. This spectral resolution of 8 cm^{-1} is consistent with the use of planar BOXCARS to obtain the propellant spectra.

The previously obtained propellant spectrum is in satisfactory agreement with calculations, properly accounting for concentration and using the Q_{32} hot band. Further measurements of M31 and similar propellants are planned. These propellants would have a flame temperature near 2,500 K and N_2 concentration near 30%. The 10^2-10^3 counts per shot obtained in the 2,000 K propane/air flame would be reduced by a factor of 2.5 by an increase of temperature to 2,500 K and a factor of 4 by a decrease of N_2 concentration to 30% to give an overall order of magnitude reduction in signal which would still be adequate for making measurements. CH_4/N_2O and other similar flames will be studied to aid in interpretation of the propellant flames.

CONCLUSIONS

Nitrogen CARS spectra from air/ar mixtures with N_2 present at concentrations from 1% to 100% air changed substantially with concentration but agreed well with calculated spectra. Nitrogen CARS spectra from propane/air flames of various equivalence ratios showed a resolved second hot band, Q_{32}, and the presence of the third hot band, Q_{43}. Temperatures determined from Q_{32} were in accord, within experimental error, with those determined from the first hot band, Q_{21}. Temperature trends for the various equivalence ratios agreed with the predictions of NASA-LEWIS thermochemical-calculations. The correlation with thermochemical-chemical calculations allowed the accuracy of the experimental measurements to be assessed at better than 5%. Nonplanar BOXCARS gave spectra similar, within experimental error, to that obtained using planar BOXCARS, thus verifying previous work employing planar BOXCARS. Calculations at near the temperature of propellant flames are similar to propellant flame spectra previously obtained at the 10% concentration expected from thermochemical calculations. The calculated spectra show the presence of Q_{32} near 30% maximum intensity as seen in the experimental propellant spectra.

REFERENCES

1. L. E. Harris and M. McIlwain, "CARS Spectroscopy of Gun Propellant Flames," Fast Reactions in Energetic Systems, ed. C. Capellos and R. F. Walker, Reidel, 1981, pp 473-484.

2. M. McIlwain and L. E. Harris, 17th JANNAF Combustion Meeting, vol II, CPIA Publication 329, 1980, pp 379-389.

3. L. E. Harris and M. McIlwain, "CARS Spectroscopy of Gun Propellant Flames," Technical Report ARLCD-TR-81007, ARRADCOM, Dover, NJ, September 1981.

4. A. C. Eckbreth and R. J. Hall, Combust. Science and Technology, vol 25, 1981, p 175.

5. R. J. Hall, Combust. Flame, vol 35, 1979, p 47.

6. R. J. Hall, Applied Spectroscopy, vol 34, 1980, p 100.

7. A. Owyoung and L. A. Rahn, IEEE, J. Quant. Elect., QE-15, 1979, pp 25D-26D.

8. A. G. Gaydon and H. G. Wolfhard, Flames, fourth edition, Chapman and Hall, London, 1979, p 324.

Table 1. Concentration of air (%) in air/ar mixtures at 300 K

*$C_{experimental}$ (%)	*$C_{calculated}$ (%)	Difference between columns 1 and 2	% Difference between columns 1 and 2
7.06	5.92	1.1	16.1
8.54	7.80	0.7	8.7
12.0	11.6	0.4	3.3
13.8	14.8	-1.0	7.2
19.7	18.8	0.9	4.5
22.8	22.7	0.1	0.50
30.2	31.0	-0.8	2.65
Mean (σ)		0.7 (0.3)	6.1 (5.1)

* Concentration

Table 2. Thermochemical calculations

Equivalence ratio	Temperature (K)	N_2 (%)	H_2O (%)	CO_2 (%)	CO (%)	H_2 (%)
0.81	2,085	73	13	10	1	-
1.01	2,273	71	15	10	2	-
1.27	2,143	67	15	7	7	3

Table 3. Temperature determined from nonplanar BOXCARS

Equivalence ratio	Temperature (K)					
	T_{21}	(σ)*	T_{32}	(σ)	T_{avg}	(σ)
0.81	1,932	(29)	1,843	(69)	1,888	(63)
1.02	2,003	(54)	1,934	(116)	1,969	(49)
1.02	1,990	(38)	1,913	(74)	1,952	(54)
1.27	1,914	(29)	1,853	(81)	1,884	(43)

Table 4. Comparison of experimental and theoretical temperatures

Equivalence ratio	Temperature (K)					
	T_{calc}	T_{21}[a]	ΔT	T_{calc}[b]	T_{21}[b]	$\%\Delta T$
1.02	2,276	1,997	279	1	1	
1.27	2,143	1,914	229	0.94	0.96	2
0.81	2,085	1,932	153	0.92	0.97	5

[a] $\Delta T = T_{cal} - T_{21}$.

[b] Normalized temperature.

Table 5. Comparison of planar and nonplanar BOXCARS temperatures

Configuration	Temperature (K)					
	T_{21}	(σ)	T_{32}	(σ)	T_{avg}	(σ)
Planar	2,021	(48)	1,902	(109)	1,962	(84)
Nonplanar	1,990	(38)	1,913	(74)	1,952	(54)

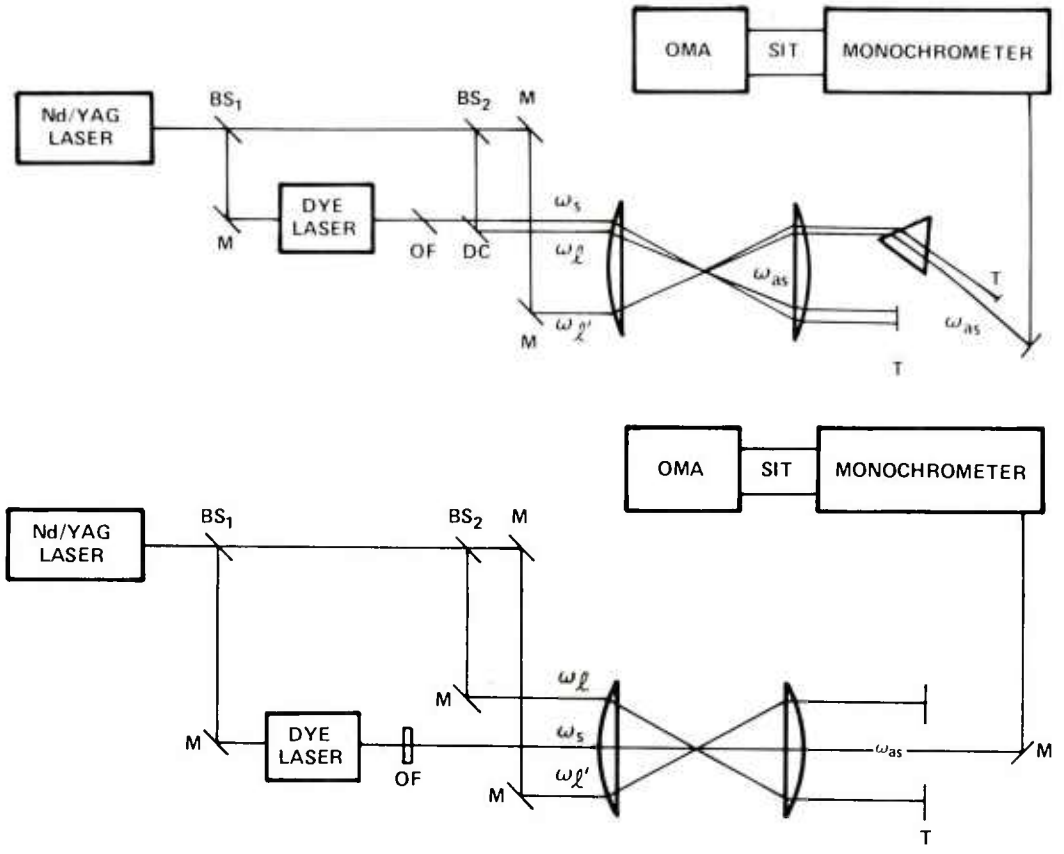

Figure 1. Phase matching

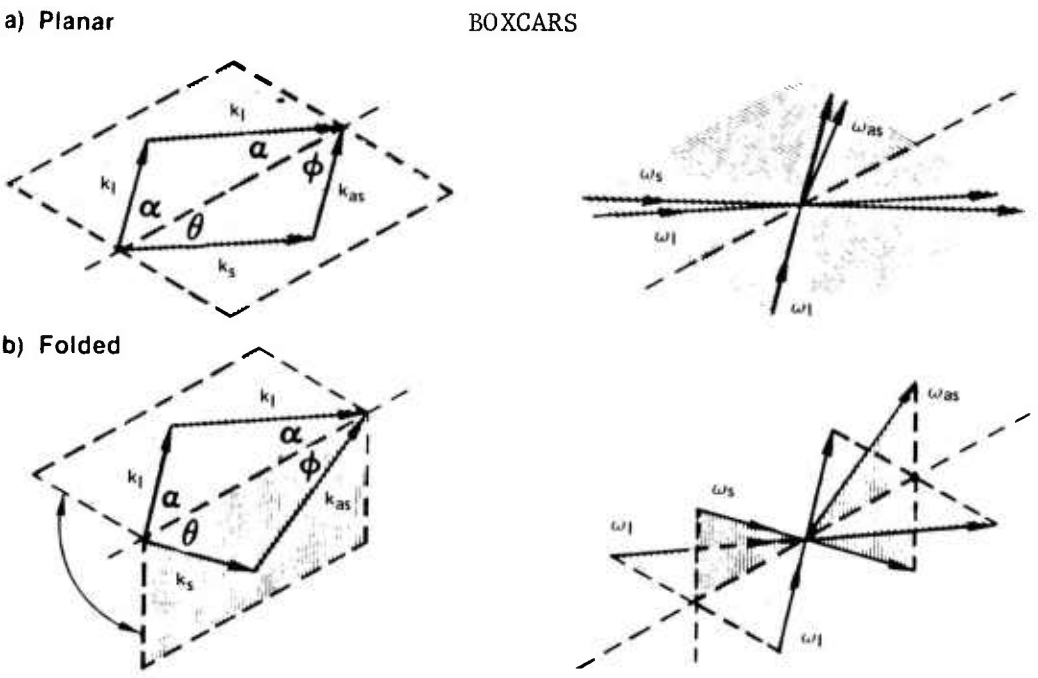

Figure 2. CARS spectrometer

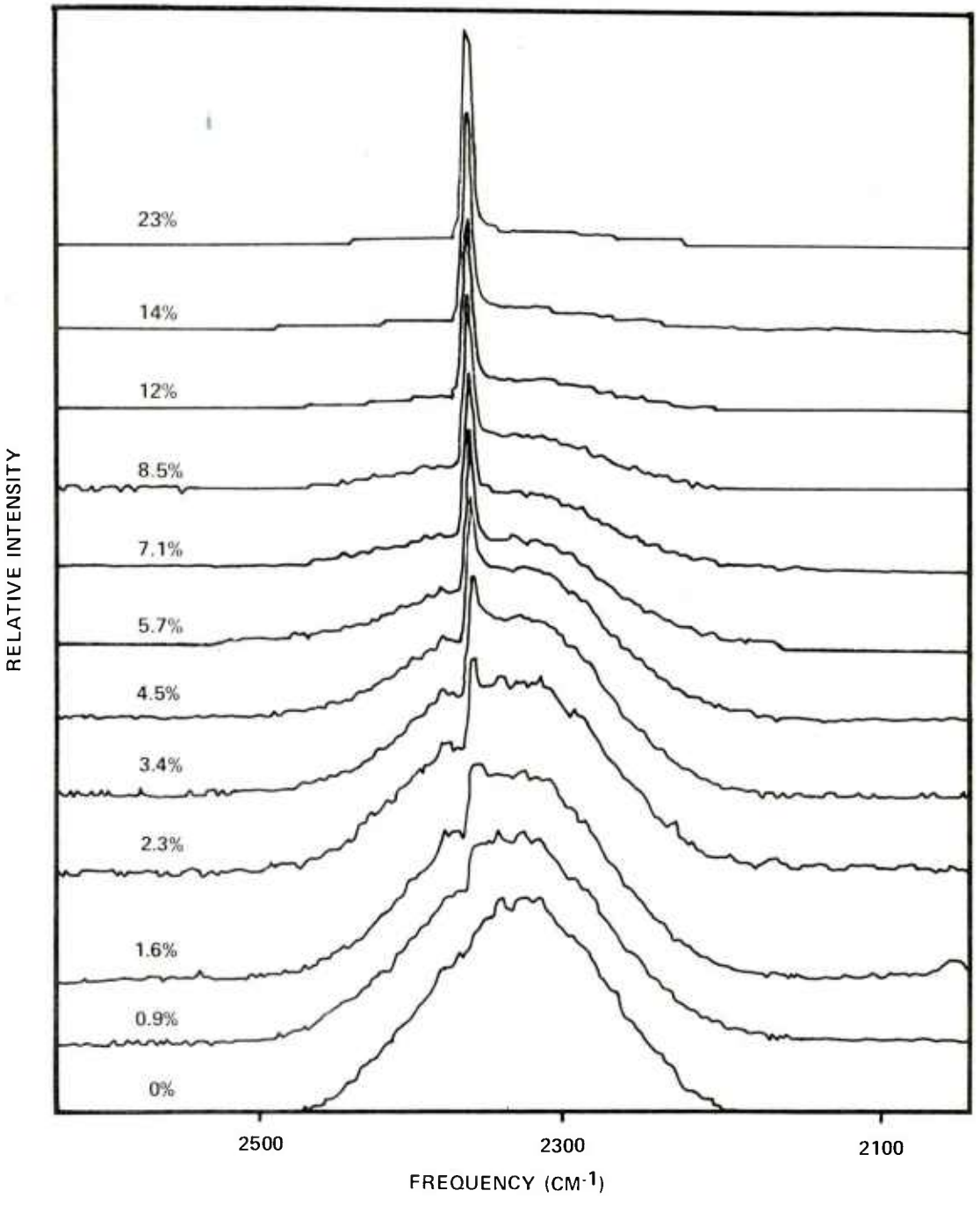

Figure 3. Normalized nitrogen CARS spectra from room temperature air/argon mixture containing 0% to 23% air

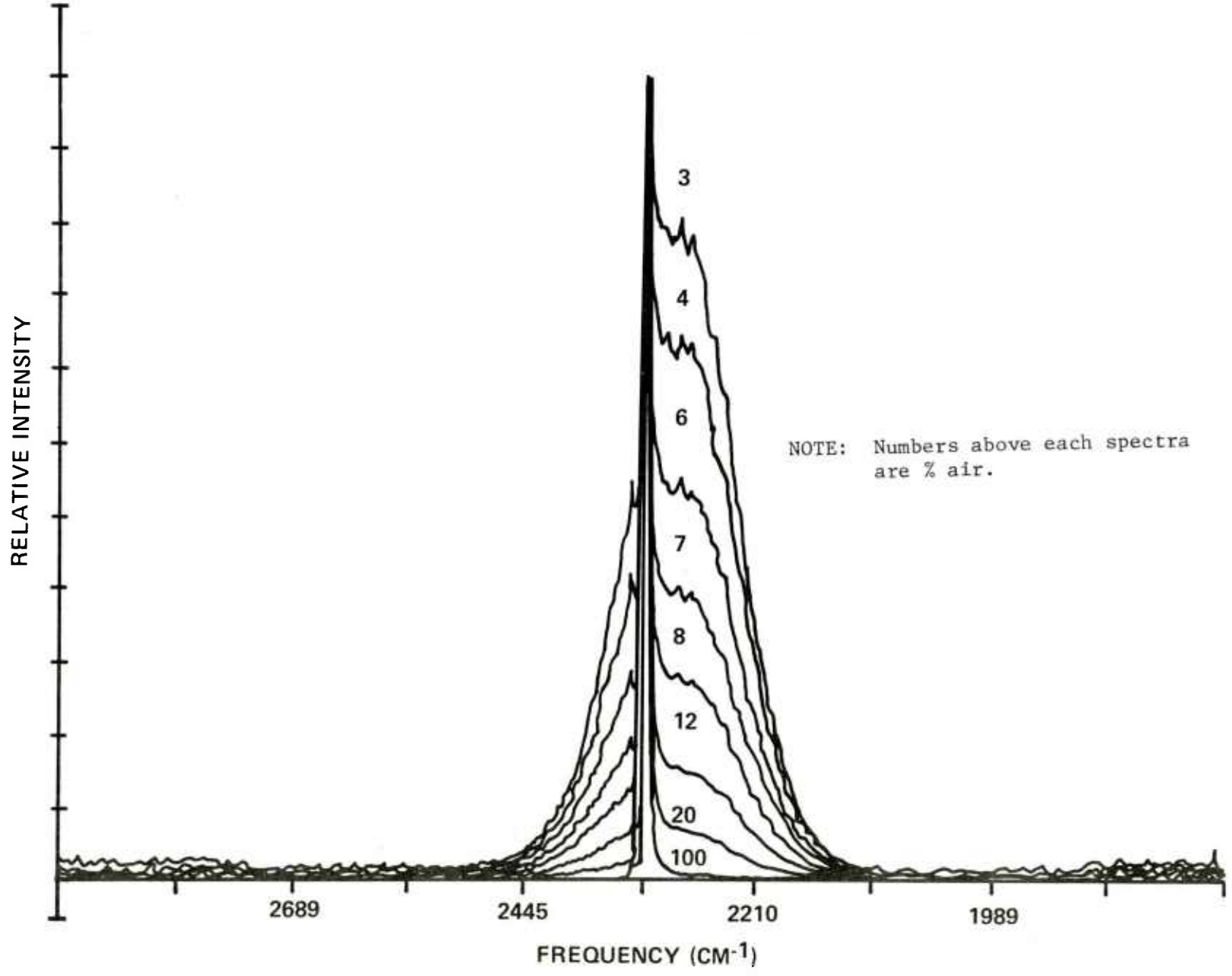

Figure 4. Normalized nitrogen CARS spectra from room temperature air/argon mixtures containing 3% to 100% air

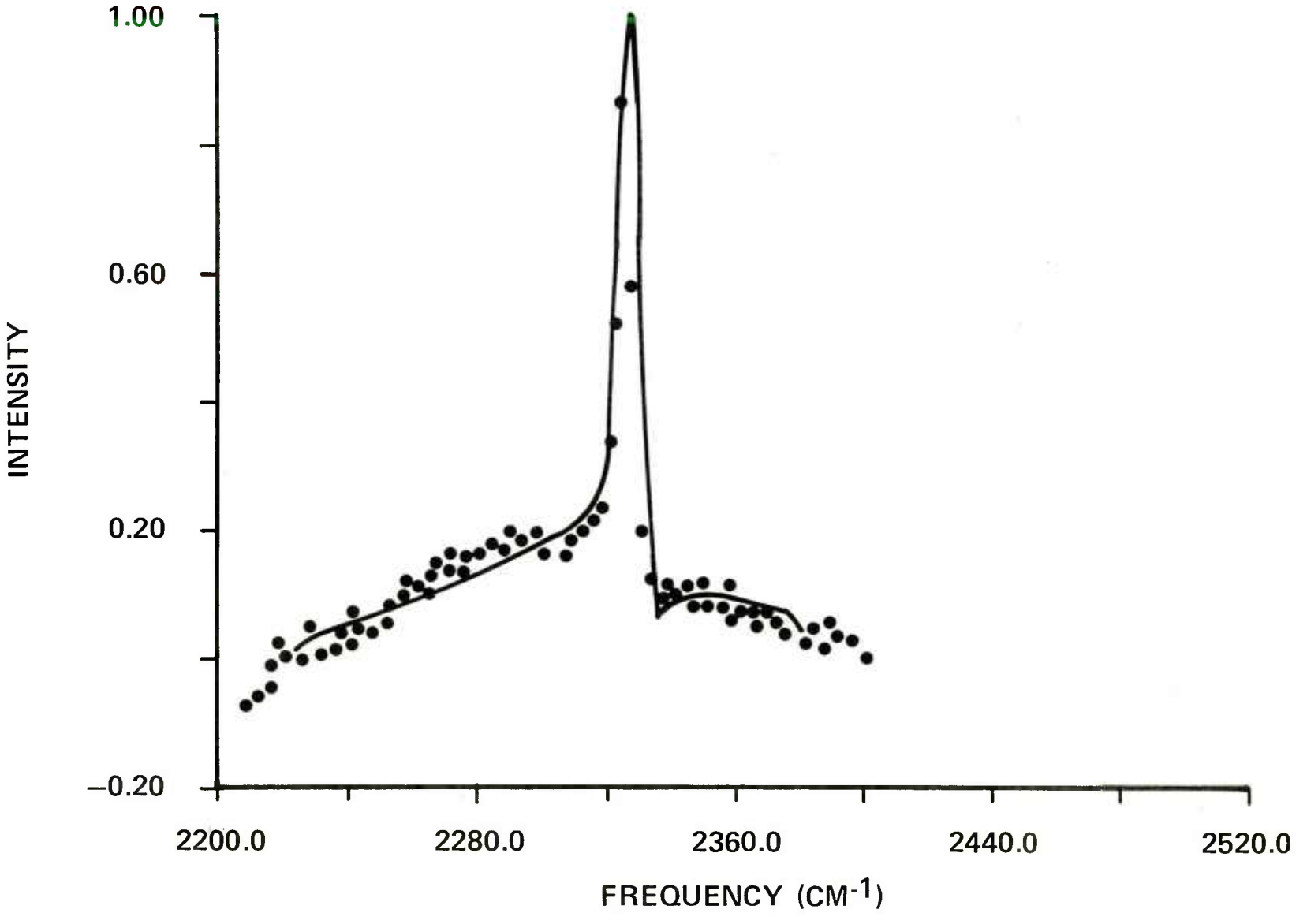

Figure 5. Experimental (.) and calculated N_2 CARS spectra at room temperature in a 9% air/argon mixture (nonplanar CARS)

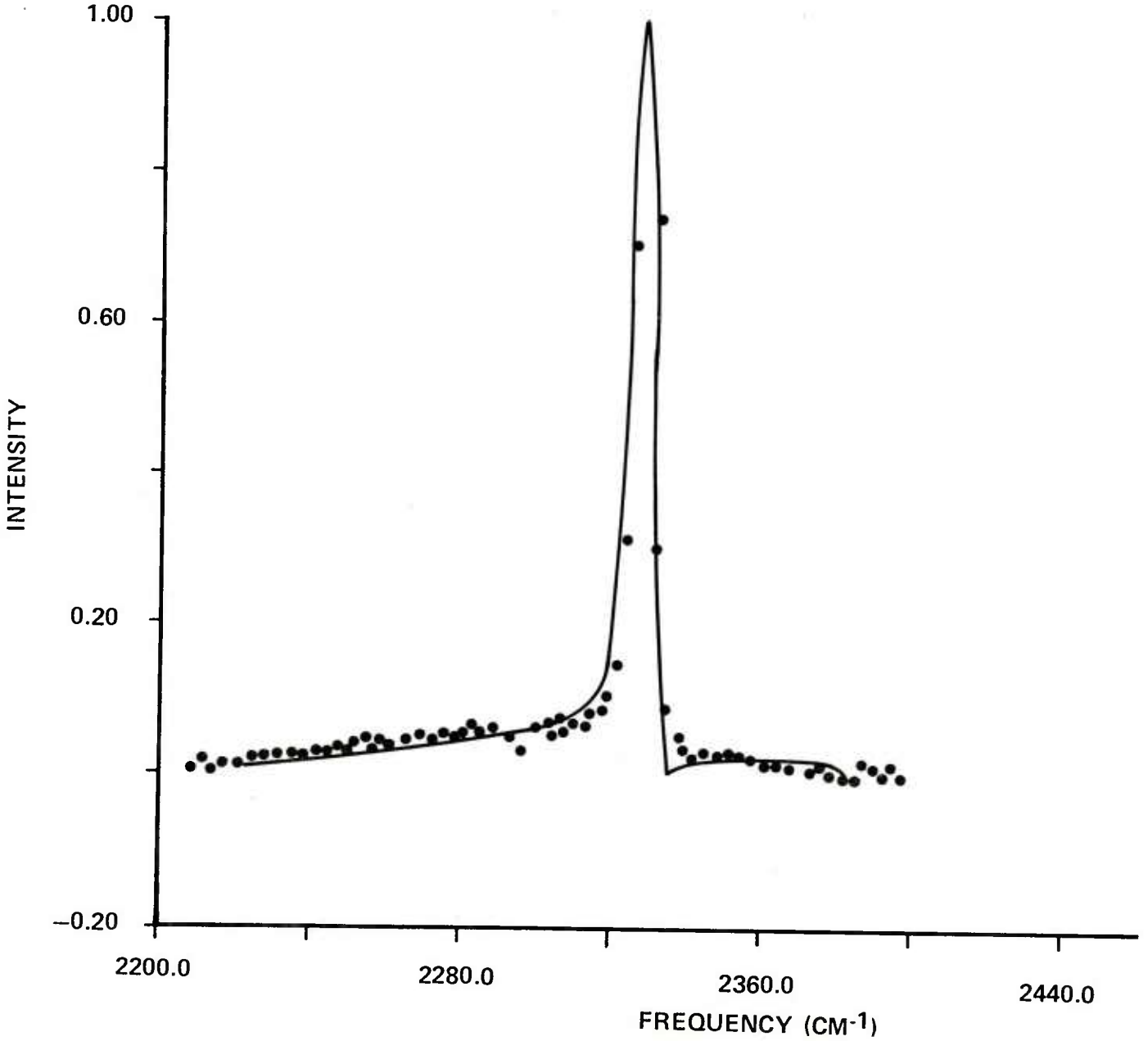

Figure 6. Experimental (.) and calculated N_2 CARS spectra at room temperature in a 20% air/argon mixture (nonplanar CARS)

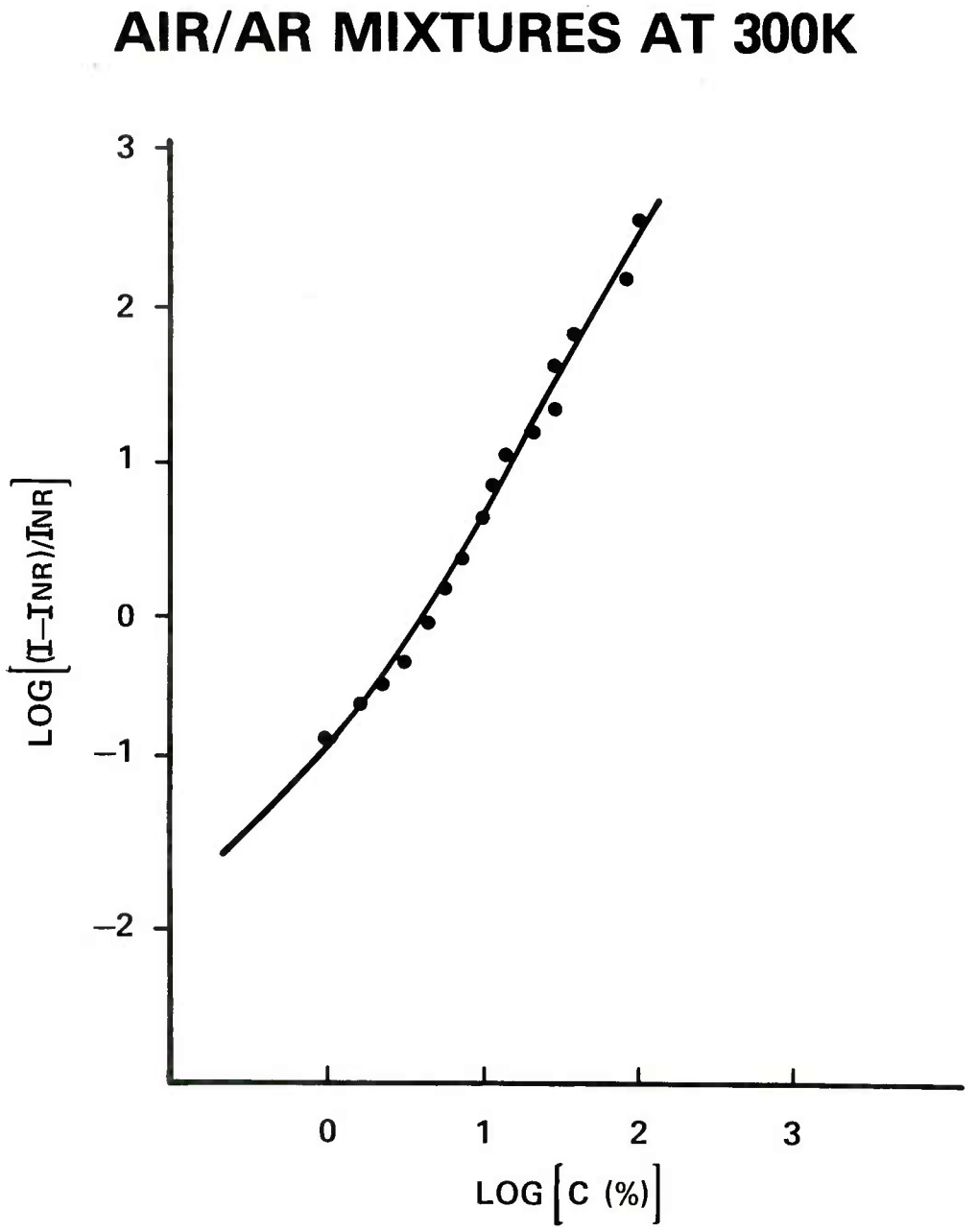

Figure 7. Experimental (.) and theoretical log $[(I_{10} - I_{NR})/I_{NR}]$ where I_{10} and I_{NR} are the maximum intensities of nitrogen Q_{10} and the nonresonant susceptibility versus log [C(%)]

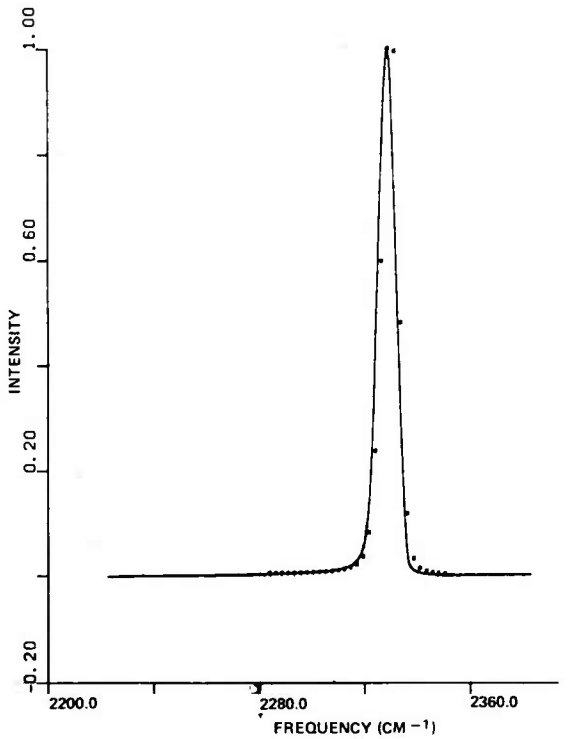

Figure 8. Experimental (.) and calculated N_2 CARS spectra of room temperature air (nonplanar CARS)

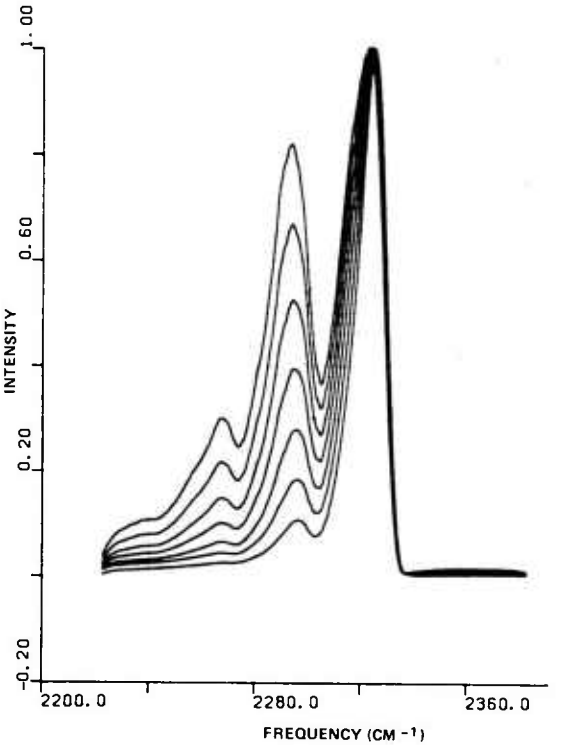

Figure 9. Calculated N_2 CARS spectra with temperature varying from 1,500 - 3,000 K at 250 K intervals

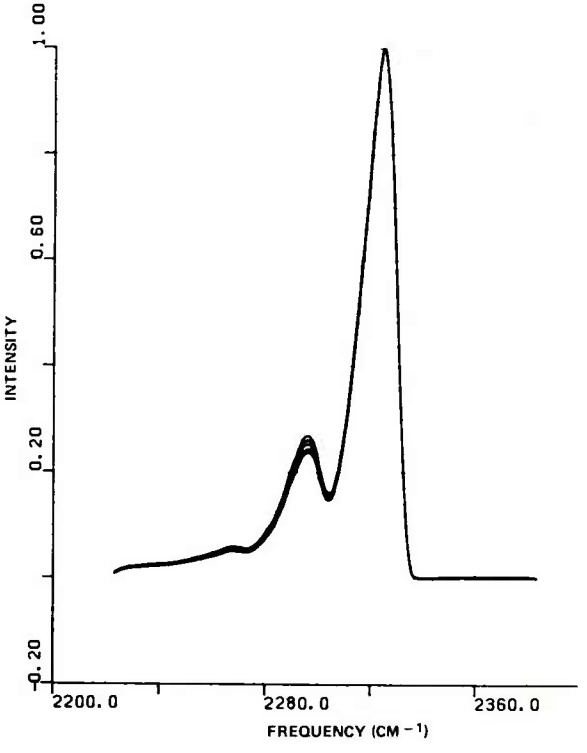

Figure 10. Calculated N_2 CARS spectra with temperature varying from 1,900 - 2,000 K at 20 K intervals

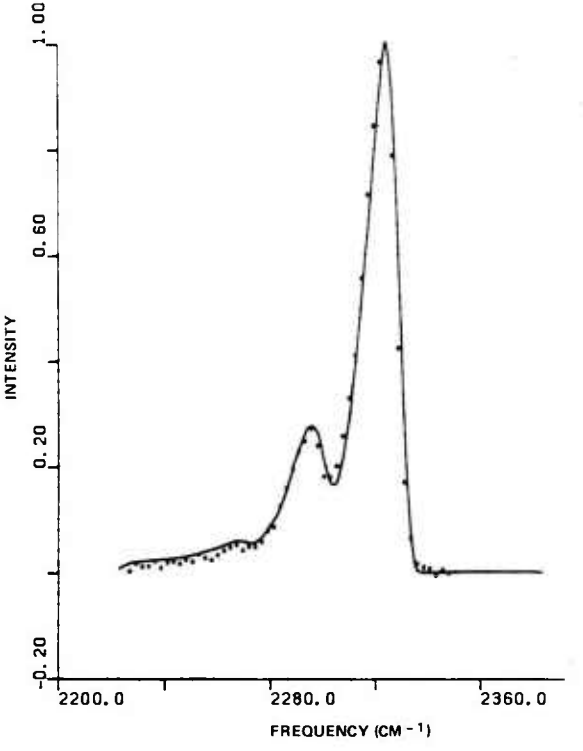

Figure 11. Experimental (.) and calculated N_2 CARS spectra for 1.02 equivalence ratio propane/air flame at T = 2,000 K (nonplanar CARS)

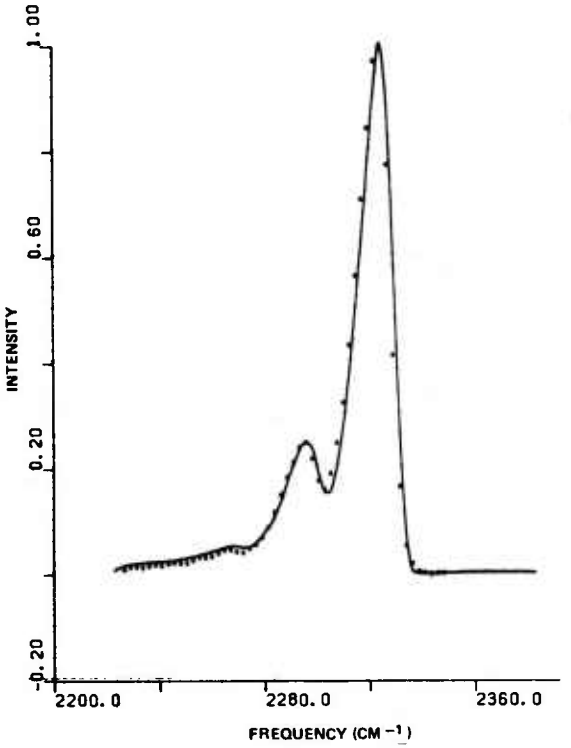

Figure 12. Experimental (.) and calculated N_2 CARS spectra for 0.81 equivalence ratio propane/air flame at T = 1,930 K (nonplanar CARS)

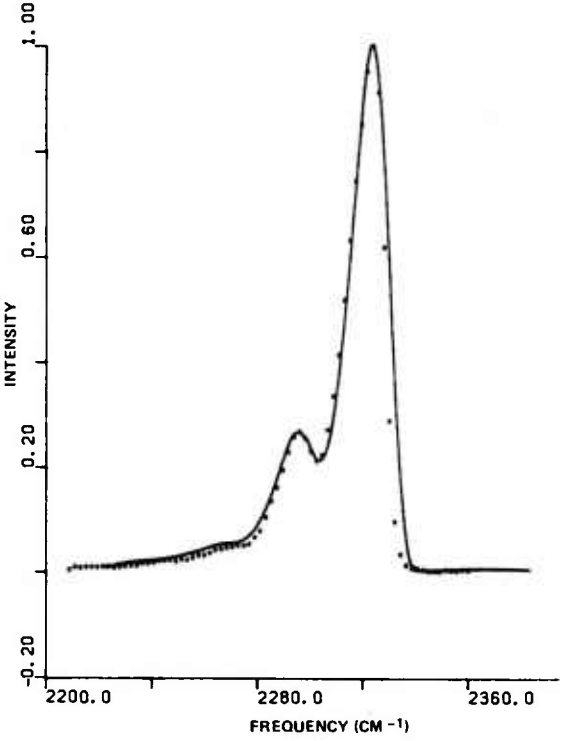

Figure 13. Experimental (.) and calculated N_2 CARS spectra for 1.02 equivalence ratio propane air flame at T = 2,020 K (planar CARS)

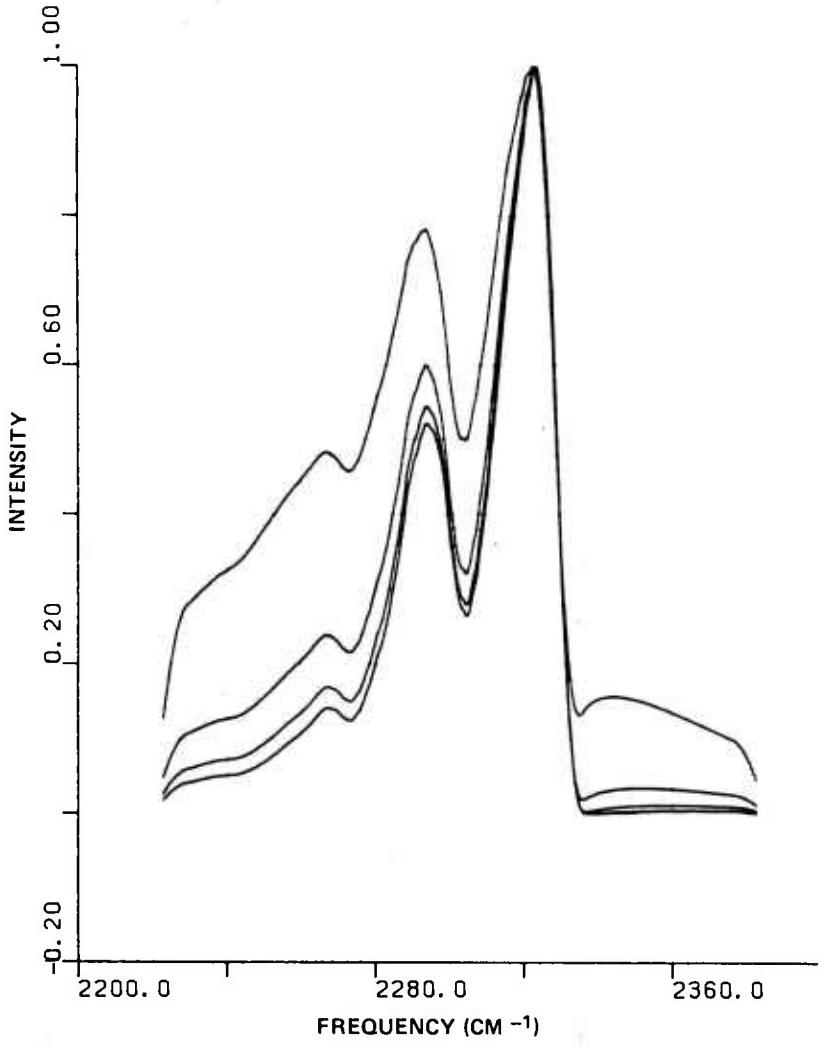

Figure 14. Calculated N_2 CARS spectra at 2,500 K for flame products with 25, 50, 70, and 100% of the stoichiometric percentage of air

DISTRIBUTION LIST

Administrator
Defense Technical Information Center
ATTN: Accessions Division (12)
Cameron Station
Alexandria, VA 22314

Director
Defense Advanced Research Projects Agency
ATTN: LTC C. Buck
1400 Wilson Boulevard
Arlington, VA 22209

Director
Institute for Defense Analyses
ATTN: H. Wolfhard
R. T. Oliver
400 Army-Navy Drive
Arlington, VA 22202

Commander
U.S. Army Materiel Development
and Readiness Command
ATTN: DRCDMD-ST
5001 Eisenhower Avenue
Alexandria, VA 22333

Commander
U.S. Army Armament Research
and Development Command
ATTN: DRDAR-TSS (5)
DRDAR-GCL
DRDAR-LC, J. Frasier
DRDAR-LCA, A. Moss
DRDAR-LCA-G, J. Lannon
D. Downs
L. Harris (10)
T. Vladimiroff
A. Beardell
Y. Carignon
DRDAR-LCE, R. Walker
P. Marinkas
C. Capellos
F. Owens
Dover, NJ 07801

Commander
U.S. Army Armament Materiel
Readiness Command
ATTN: DRSAR-LEP-L
Rock Island, IL 61299

Chief
Benet Weapons Laboratory, LCWSL
U.S. Army Armament Research
and Development Command
ATTN: DRDAR-LCB-TL
Watervliet, NY 12189

Commander
U.S. Army Watervliet Arsenal
ATTN: SARWV-RD, R. Thierry
Watervliet, NY 12189

Commander
U.S. Army Aviation Research
and Development Command
ATTN: DRSAV-E
P.O. Box 209
St. Louis, MO 63166

Director
U.S. Army Air Mobility Research
and Development Laboratory
Ames Research Center
Moffett Field, CA 94035

Commander
U.S. Army Communications Research
and Development Command
ATTN: DRDCO-PPA-SA
Fort Monmouth, NJ 07703

Commander
U.S. Army Electronics Research
and Development Command
Technical Support Activity
ATTN: DELSD-L
Fort Monmouth, NJ 07703

Commander
U.S. Army Missile Command
ATTN: DRSMI-R
DRSMI-YDL
Redstone Arsenal, AL 35809

Commander
U.S. Army Natick Research
and Development Command
ATTN: DRXRE, D. Sieling
Natick, MA 01762

Commander
U.S. Army Tank Automotive Research
and Development Command
ATTN: DRDTA-UL
Warren, MI 48090

Commander
U.S. Army White Sands Missile Range
ATTN: STEWS-VT
White Sands Missile Range, NM 88002

Commander
U.S. Army Materials and
Mechanics Research Center
ATTN: DRXMR-ATL
Watertown, MA 02172

Commander
U.S. Army Research Office
ATTN: Technical Library
D. Squire
F. Schmiedeshaff
R. Ghirardelli
M. Ciftan
P.O. Box 12211
Research Triangle Park, NC 27706

Director
U.S. Army TRADOC Systems
Analysis Activity
ATTN: ATAA-SL
White Sands Missile Range, NM 88002

Office of Naval Research
ATTN: Code 473
G. Neece
800 N. Quincy Street
Arlington, VA 22217

Commander
Naval Sea Systems Command
ATTN: J. W. Murrin, SEA-62R2
National Center
Bldg 2, Room 6E08
Washington, DC 20362

Commander
Naval Surface Weapons Center
ATTN: Library Branch, DX-21
Dahlgren, VA 22448

Commander
Naval Surface Weapons Center
ATTN: Code 240, S. J. Jacobs
Code 730
Silver Spring, MD 20910

Commander
Naval Underwater Systems Center
Energy Conversion Department
ATTN: Code 5B331, R. S. Lazar
Newport, RI 02840

Commander
Naval Weapons Center
ATTN: R. Derr
C. Thelen
China Lake, CA 93555

Commander
Naval Research Laboratory
ATTN: Code 6180
Washington, DC 20375

Superintendent
Naval Postgraduate School
ATTN: Technical Library
D. Netzer
A. Fuhs
Monterey, CA 93940

Commander
Naval Ordnance Station
ATTN: Dr. Charles Dale
Technical Library
Indian Head, MD 20640

AFOSR
ATTN: J. F. Masi
B. T. Wolfson
D. Ball
L. Caveny
Bolling AFB, DC 20332

AFRPL (DYSC)
ATTN: D. George
J. N. Levine
Edwards AFB, CA 93523

National Bureau of Standards
ATTN: J. Hastie
T. Kashiwagi
Washington, DC 20234

Lockheed Palo Alto Research Laboratories
ATTN: Technical Information Center
3521 Hanover Street
Palo Alto, CA 94304

Aerojet Solid Propulsion Co.
ATTN: P. Micheli
Sacramento, CA 95813

ARO Incorporated
ATTN: N. Dougherty
Arnold AFS, TN 37389

Atlantic Research Corporation
ATTN: M. K. King
5390 Cherokee Avenue
Alexandria, VA 22314

AVCO Corporation
AVCO Everett Research Laboratory Division
ATTN: D. Stickler
2385 Revere Beach Parkway
Everett, MA 02149

Calspan Corporation
ATTN: E. B. Fisher
A. P. Trippe
P.O. Box 400
Buffalo, NY 14221

Foster Miller Associates, Inc.
ATTN: A. J. Erickson
135 Second Avenue
Waltham, MA 02154

General Electric Company
Armament Department
ATTN: M. J. Bulman
Lakeside Avenue
Burlington, VT 05402

General Electric Company
Flight Propulsion Division
ATTN: Technical Library
Cincinnati, OH 45215

Hercules Incorporated
Alleghany Ballistic Lab
ATTN: R. Miller
Technical Library
Cumberland, MD 21501

Hercules Incorporated
Bacchus Works
ATTN: B. Isom
Magna, UT 84044

IITRI
ATTN: M. J. Klein
10 West 35th Street
Chicago, IL 60615

Olin Corporation
Badger Army Ammunition Plant
ATTN: J. Ramnarace
Baraboo, WI 53913

Olin Corporation
New Haven Plant
ATTN: R. L. Cook
D. W. Riefler
275 Winchester Avenue
New Haven, CT 06504

Paul Gough Associates, Inc.
ATTN: P. S. Gough
P.O. Box 1614
Portsmouth, NH 03801

Physics International Company
2700 Merced Street
Leandro, CA 94577

Pulsepower Systems, Inc.
ATTN: L. C. Elmore
815 American Street
San Carlos, CA 94070

Rockwell International Corp.
Rocketdyne Division
ATTN: C. Obert
J. E. Flanagan
A. Axeworthy
6633 Canoga Avenue
Canoga Park, CA 91304

Rockwell International Corp.
Rocketdyne Division
ATTN: W. Haymes
Technical Library
McGregor, TX 76657

Science Applications, Inc.
ATTN: R. B. Edelman
Combustion Dynamics and
Propulsion Division
23146 Cumorah Crest
Woodland Hills, CA 91364

Shock Hydrodynamics, Inc.
ATTN: W. H. Anderson
4710-16 Vineland Avenue
N. Hollywood, CA 91602

Thiokol Corporation
Elkton Division
ATTN: E. Sutton
Elkton, MD 21921

Thiokol Corporation
Huntsville Division
ATTN: D. Flanigan
R. Glick
Technical Library
Huntsville, AL 35807

Thiokol Corporation
Wasatch Division
ATTN: J. Peterson
Technical Library
P.O. Box 524
Brigham City, UT 84302

TRW Systems Group
ATTN: H. Korman
One Space Park
Redondo Beach, CA 90278

United Technologies
Chemical Systems Division
ATTN: R. Brown
Technical Library
P.O. Box 358
Sunnyvale, CA 94086

Universal Propulsion Co.
ATTN: H. J. McSpadden
1800 W. Deer Valley road
Phoenix, AZ 85027

Battelle Memorial Institute
ATTN: Technical Library
R. Bartlett
505 King Avenue
Columbus, OH 43201

Brigham Young University
Department of Chemical Engineering
ATTN: M. W. Beckstead
Provo, UT 84601

California Institute of Technology
204 Karmar Lab
Mail Stop 301-46
ATTN: F. E. C. Culick
1201 E. California Street
Pasadena, CA 91125

Case Western Reserve University
Division of Aerospace Sciences
ATTN: J. Tien
Cleveland, OH 44135

Georgia Institute of Technology
School of Aerospace Engineering
ATTN: B. T. Zinn
E. Price
W. C. Strahle
Atlanta, GA 30332

Institute of Gas Technology
ATTN: D. Gidaspow
3424 S. State Street
Chicago, IL 60616

Johns Hopkins University/APL
Chemical Propulsion Information Agency
ATTN: T. Christian
Johns Hopkins Road
Laurel, MD 20810

Massachusetts Institute of Technology
Department of Mechanical Engineering
ATTN: T. Toong
Cambridge, MA 02139

Pennsylvania State University
Applied Research Laboratory
ATTN: G. M. Faeth
P.O. Box 30
State College, PA 16801

Pennsylvania State University
Department of Mechanical Engineering
ATTN: K. Kuo
Universtiy Park, PA 16801

Pennsylvania State University
Department of Material Sciences
ATTN: H. Palmer
University Park, PA 16801

Princeton Combustion Research Laboratories
ATTN: M. Summerfield
1041 U.S. Highway One North
Princeton, NJ 08540

Princeton University
Forrestal Campus
ATTN: I. Glassman
Technical Library
P.O. Box 710
Princeton, NJ 08540

Purdue University
School of Mechanical Engineering
ATTN: J. Osborn
S. N. B. Murthy
TSPC Chaffee Hall
W. Lafayette, IN 47906

Rutgers State University
Department of Mechanical and
Aerospace Engineering
ATTN: S. Temkin
University Heights Campus
New Brunswick, NJ 08903

SRI International
ATTN: Technical Library
D. Crosley
J. Barker
D. Golden
333 Ravenswood Avenue
Menlo Park, CA 94025

Stevens Institute of Technology
Davidson Library
ATTN: R. McAlevy, III
Hoboken, NJ 07030

United Technology
ATTN: Alan Ecbreth
Research Center
East Hartford, CT 06108

Director
U.S. Army Materiel Systems
Analysis Activity
ATN: DRXSY-MP
Aberdeen Proving Ground, MD 21005

Commander/Director
Chemical Systems Laboratory
U.S. Army Armament Research
and Development Command
ATTN: DRDAR-CLJ-L
DRDAR-CLB-PA
APG, Edgewood Area, MD 21010

Director
Ballistics Research Laboratory
U.S. Army Armament Research
and Development Command
ATTN: DRDAR-TSB-S
DRDAR-BLP, L. Watermier
A. Barrows
C. Nelson
J. Vanderhoff
J. Anderson
Aberdeen Proving Ground, MD 21005